

UNIVERSIDADE ESTADUAL DE CAMPINAS
SISTEMA DE BIBLIOTECAS DA UNICAMP
REPOSITÓRIO DA PRODUÇÃO CIENTÍFICA E INTELLECTUAL DA UNICAMP

Versão do arquivo anexado / Version of attached file:

Versão do Editor / Published Version

Mais informações no site da editora / Further information on publisher's website:

<https://ieeexplore.ieee.org/abstract/document/7378969>

DOI: 10.1109/TMAG.2016.2517127

Direitos autorais / Publisher's copyright statement:

©2016 by Institute of Electrical and Electronics Engineers. All rights reserved.

DIRETORIA DE TRATAMENTO DA INFORMAÇÃO

Cidade Universitária Zeferino Vaz Barão Geraldo

CEP 13083-970 – Campinas SP

Fone: (19) 3521-6493

<http://www.repositorio.unicamp.br>

Analytic and Experimental Analysis of Magnetic Force Equations

Sergio Gama¹, Lucas D. R. Ferreira², Carlos V. X. Bessa², Oswaldo Horikawa², Adelino A. Coelho³, Flávio C. Gandra³, Raul Araujo⁴, and Peter W. Egolf⁴

¹Federal University of São Paulo, Diadema 09913-030, Brazil

²Department of Mechanical Engineering, Polytechnic School, University of São Paulo, São Paulo 05508-030, Brazil

³University of Campinas, Campinas 13083-859, Brazil

⁴Thermal Sciences and Engineering Institute, University of Applied Sciences, Yverdon-les-Bains 1401, Switzerland

The design of magnetic devices requires a precise estimation of magnetic forces. In previous works, we presented a general approach to estimate these forces based upon thermodynamically closed systems, resulting in four different forms of the force equations. This paper presents a complete theoretical model analysis tested by experiments, using arrangements of permanent magnets and a device for measuring the force induced on a soft magnetic material according to its position with respect to the permanent magnets. The results of analytical formulation, Finite Element Method numerical analysis, and experiments are compared with each other. This enabled the identification of two forms of the force equations that most precisely describe the magnetic forces. A follow-up experiment is then proposed and executed, identifying the correct form of the magnetic force equations. The resulting equation can be used to analytically estimate the magnetic force in many practical problems.

Index Terms—Experimental validation, magnetic analysis, magnetic forces, permanent magnets.

I. INTRODUCTION

THE proper estimate and the knowledge of the correct magnetic forces with their direct relations to their specific energies are very important for designing magnetic, electromagnetic, and magnetocaloric devices [1], [2]. This knowledge results in equations that enable a precise prediction of magnetic forces and, consequently, more efficient magnetic devices. Along the past works, we presented four variants of force equations, and this paper aims to identify those that correctly describe the magnetic force.

Magnetic forces can be explained by analogy with the conventional thermodynamic analysis of gases. The pressure (p) of the gas is equivalent to the magnetic applied field (H), and the specific volume (v) of the gas is analog to the magnetization (M) of the magnetic material. Depending on the system, the specific work (w) in a gas thermodynamic analysis can be calculated by $p dv$ or $v dp$. In an analog magnetic system, the specific work can be defined as $\mu_0 H dM$ (related to force of Liu) or $\mu_0 M dH$ (related to the Kelvin force) [3], where μ_0 is the vacuum permeability.

From the equations of this paper, it is possible to derive the magnetic force, and (1)–(4) are possible representations of the magnetic specific force, as shown in [3] and [4]. In the equations, H_{ext} is the external applied field, and H_{int} is the field inside of a magnetic material

$$f_1 = \mu_0 \begin{pmatrix} H_{\text{ext}_x} \frac{\delta}{\delta x} M_x & H_{\text{ext}_y} \frac{\delta}{\delta x} M_y & H_{\text{ext}_z} \frac{\delta}{\delta x} M_z \\ H_{\text{ext}_x} \frac{\delta}{\delta y} M_x & H_{\text{ext}_y} \frac{\delta}{\delta y} M_y & H_{\text{ext}_z} \frac{\delta}{\delta y} M_z \\ H_{\text{ext}_x} \frac{\delta}{\delta z} M_x & H_{\text{ext}_y} \frac{\delta}{\delta z} M_y & H_{\text{ext}_z} \frac{\delta}{\delta z} M_z \end{pmatrix} \quad (1)$$

$$f_2 = \mu_0 \begin{pmatrix} H_{\text{int}_x} \frac{\delta}{\delta x} M_x & H_{\text{int}_y} \frac{\delta}{\delta x} M_y & H_{\text{int}_z} \frac{\delta}{\delta x} M_z \\ H_{\text{int}_x} \frac{\delta}{\delta y} M_x & H_{\text{int}_y} \frac{\delta}{\delta y} M_y & H_{\text{int}_z} \frac{\delta}{\delta y} M_z \\ H_{\text{int}_x} \frac{\delta}{\delta z} M_x & H_{\text{int}_y} \frac{\delta}{\delta z} M_y & H_{\text{int}_z} \frac{\delta}{\delta z} M_z \end{pmatrix} \quad (2)$$

$$f_3 = \mu_0 \begin{pmatrix} M_x \frac{\delta}{\delta x} H_{\text{ext}_x} & M_y \frac{\delta}{\delta x} H_{\text{ext}_y} & M_z \frac{\delta}{\delta x} H_{\text{ext}_z} \\ M_x \frac{\delta}{\delta y} H_{\text{ext}_x} & M_y \frac{\delta}{\delta y} H_{\text{ext}_y} & M_z \frac{\delta}{\delta y} H_{\text{ext}_z} \\ M_x \frac{\delta}{\delta z} H_{\text{ext}_x} & M_y \frac{\delta}{\delta z} H_{\text{ext}_y} & M_z \frac{\delta}{\delta z} H_{\text{ext}_z} \end{pmatrix} \quad (3)$$

$$f_4 = \mu_0 \begin{pmatrix} M_x \frac{\delta}{\delta x} H_{\text{int}_x} & M_y \frac{\delta}{\delta x} H_{\text{int}_y} & M_z \frac{\delta}{\delta x} H_{\text{int}_z} \\ M_x \frac{\delta}{\delta y} H_{\text{int}_x} & M_y \frac{\delta}{\delta y} H_{\text{int}_y} & M_z \frac{\delta}{\delta y} H_{\text{int}_z} \\ M_x \frac{\delta}{\delta z} H_{\text{int}_x} & M_y \frac{\delta}{\delta z} H_{\text{int}_y} & M_z \frac{\delta}{\delta z} H_{\text{int}_z} \end{pmatrix} \quad (4)$$

In this paper, the magnetic force is calculated using (1)–(4) in three different configurations of permanent magnets and ferromagnetic spheres, as shown in Fig. 1. Analytical results are then compared with experimental measurements and Finite Element Method (FEM) analysis. This procedure allowed the identification of the most correct form of the magnetic force equations. Although similar analytical formulations may be found in [3] and [4], this sort of thorough experimental comparison, to our knowledge, has not been done before.

II. THEORETICAL ANALYSIS

The analysis consisted in calculating the magnetic force in the sphere according to its position in relation to a given magnetic field. Calculations considered a 4 mm diameter sphere made of chrome steel alloy (100Cr6). Three different

Manuscript received November 5, 2015; accepted January 4, 2016. Date of publication January 12, 2016; date of current version June 22, 2016. Corresponding author: C. V. X. Bessa (e-mail: carlosviniciusxb@usp.br).

Digital Object Identifier 10.1109/TMAG.2016.2517127

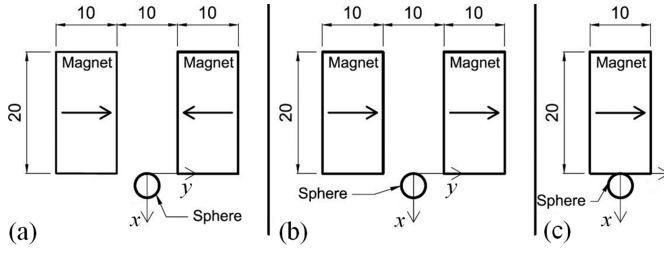


Fig. 1. Section view of the three configurations used to measure and to calculate the magnetic force at the sphere along a displacement in the x -direction. (a) Two permanent magnets arranged in a repelling configuration. (b) Two permanent magnets arranged in an attracting configuration. (c) Single permanent magnet. All dimensions are in millimeter.

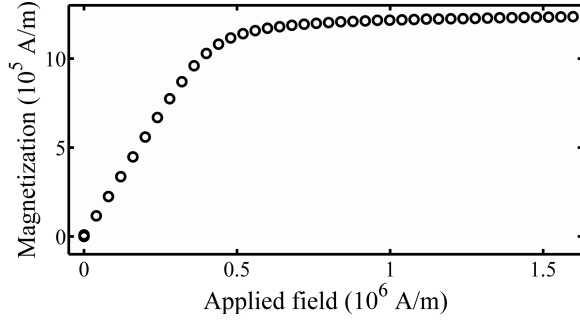


Fig. 2. Magnetization as a function of the external applied field for a sphere of 100Cr6 steel with a diameter of 4 mm.

permanent magnets arrays produced the magnetic field (permanent magnets bars with dimensions 10 mm \times 20 mm \times 100 mm and magnetic coercivity -1050000 A/m). Cross-sectional views at the middle plane of each configuration are shown in Fig. 1.

Due to the symmetric geometry of the configurations, there were no forces in the sphere in the y - and z -directions. Forces in the x -direction were calculated for the configurations using the first line of the matrix to each equation. Therefore, for each position of the sphere, it was necessary to determine the applied field as well the magnetization of the material. Engel-Herbert and Hesjedal [5] developed an analytical formulation to determine the external magnetic field distribution for one permanent magnetic bar. This formulation was extended for two permanent magnetic bars [6], thus allowing the calculation of H_{ext} at the desired positions. Using the same sphere mentioned before, M was determined using a superconducting quantum interference device magnetometer. The obtained $M(H_{\text{ext}})$ curve is shown in Fig. 2.

In a sphere, the demagnetization factor (n) is 1/3 in all directions. Moreover, due to the symmetry, M was easily calculated for any direction of the sphere. Consequently, H_{int} was readily calculated by (5), where index k denotes x -, y -, or z -directions

$$H_{\text{int}_k} = H_{\text{ext}_k} - n_k M_k. \quad (5)$$

On using force equations, some approximations become necessary. The approximations of the derivatives of H and M along the positions are given, respectively, by (6) and (7). The values of H and M were calculated for each position of

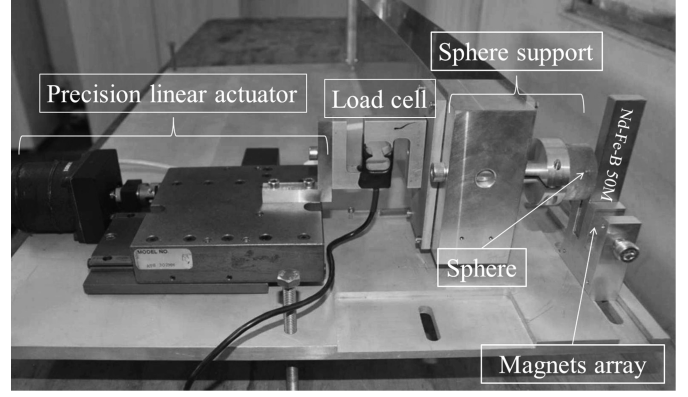


Fig. 3. Device for force measurement as a function of position.

the sphere using (8) and (9). The subscript in these equations indicates the position, where variable H or M was calculated. C is the position of the center of the sphere, and r is its radius

$$\frac{\partial H}{\partial x} \cong \frac{H_{C+r} - H_{C-r}}{2r} \quad (6)$$

$$\frac{\partial M}{\partial x} \cong \frac{M_{C+r} - M_{C-r}}{2r} \quad (7)$$

$$H \cong \frac{H_{C+r} + H_{C-r}}{2} \quad (8)$$

$$M \cong \frac{M_{C+r} + M_{C-r}}{2}. \quad (9)$$

III. DESCRIPTION OF THE EXPERIMENTS

In order to verify the equations, two experiments were conducted. The first one used the configurations shown in Fig. 1(a)–(c). Results obtained here were compared with the analytical ones. The second experiment verified the contribution of the magnetization gradient to the force. This effect is predicted by (1) and (2).

A. Experiment 1—Direct Verification of the Equations

Fig. 3 shows the device used in the measurement of the magnetic force. The system consists of: 1) a precision linear actuator that moves a 4 mm diameter 100Cr6 steel sphere; 2) a position sensor, which measures the position of the sphere under a resolution of 0.07 mm of precision; 3) the magnetic field is produced by Nd–Fe–B 50 M permanent magnets with dimensions 10 mm \times 20 mm \times 100 mm. The magnetic array is interchangeable, and this way it is possible to test the three proposed configurations; and 4) a load cell able to measure up to 50 N with a precision of ± 0.05 N measured the magnetic force on the sphere as a function of its position along the displacement direction (x -axis), which is located in the central position regarding the magnets. A schematic view of this device is shown in Fig. 4.

The load cell has a setting time that does not permit a continuous measurement. Each time the linear actuator displaced the sphere 0.28 mm, the actuator was stopped, the load cell output was read after waiting a few seconds so as to assure the correct measurement was recorded, and then the sphere was displaced again and a new measurement executed.

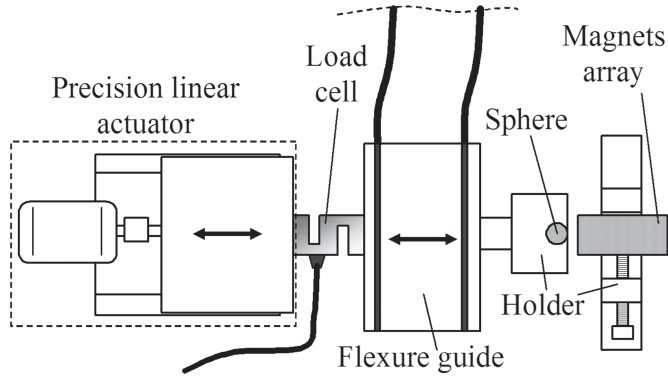


Fig. 4. Schematic view of the device for force measurement as a function of position.

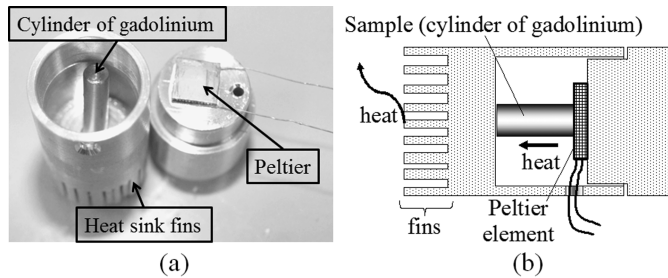


Fig. 5. Apparatus to provide a constant gradient of temperature in the gadolinium. (a) Disassembled system. (b) Schematic view.

B. Experiment 2—Verification of the Magnetic Force in a Constant Applied Field

Using the thermomagnetic effect, i.e., the influence of the temperature on the material magnetization [7], [8], it is possible to have a continuous magnetization gradient in a body placed in a region subjected to a constant magnetic applied field. Such situation is ideal to verify (1) and (2). The magnetization gradient is intensified when the temperature of the material increases above its Curie temperature (T_C) and changes its magnetic state from ferromagnetic to paramagnetic [9], [10].

In the second experiment, we submit a cylindrical sample of gadolinium (2 mm × 20 mm) to a linear gradient of temperature. For this, a Peltier element inserted between the Gd and the aluminum body was used as a heat pump, providing a constant heat flow to the Gd sample. The heat flux establishes a temperature gradient on the sample and is then rejected to the sample chamber of a physical property measurement system (PPMS) with controlled temperature. In this way, a thermal steady-state condition of the gadolinium cylinder was assured. The disassembled system is shown in Fig. 5(a), and a schematic view is shown in Fig. 5(b).

The temperature difference between the two extremities of the Gd sample was close to 20 K, and the PPMS sample chamber was set to a temperature close to the gadolinium T_C (~293 K). This ensured a strong and continuous magnetization gradient inside the material. In the sample region, a superconducting magnet provided a uniform field of 5 T with high homogeneity. The cylinder was suspended

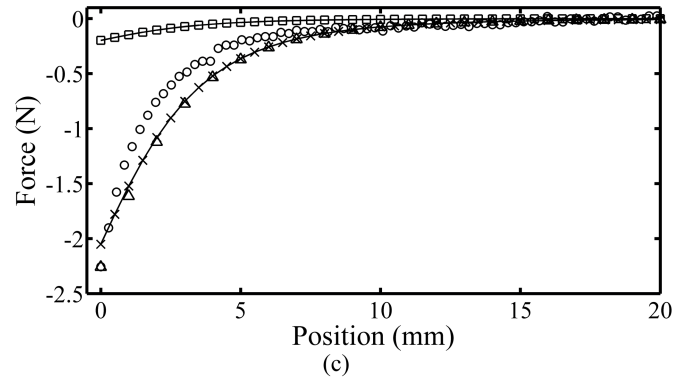
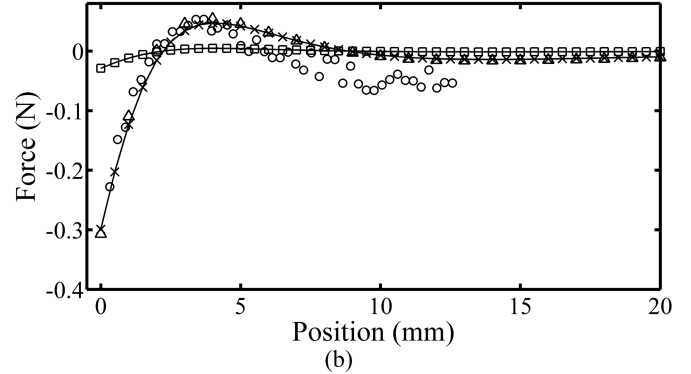
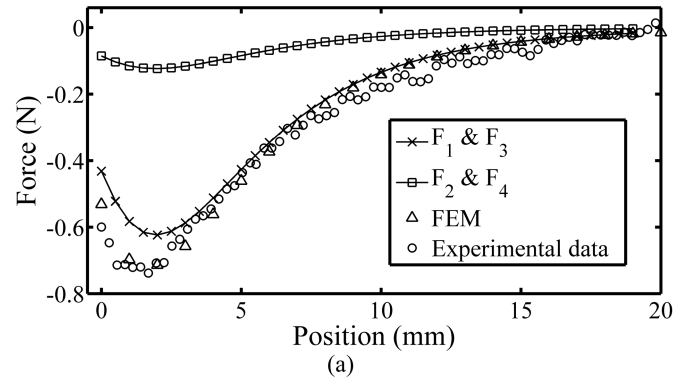


Fig. 6. Analytical, experimental, and computational simulations results for the three configurations. (a) Force in the displacement direction to “configuration a.” (b) Force in the displacement direction to “configuration b.” (c) Force in the displacement direction to “configuration c.”

in an analytical balance able to measure up to 2 N with a precision of 0.001 N to measure the magnetic force.

IV. RESULTS

A. Experiment 1

To compare analytical results with experimental ones, (1)–(4) were multiplied by the volume of the sphere, converting the specific force (N/m³) into force (N). Analytical and experimental results are shown in Fig. 6. This figure also shows the results of FEM analysis (Ansoft Maxwell 3D V. 14.0.0) based on Maxwell’s equations. F_1 , F_2 , F_3 , and F_4 are the results from (1), (2), (3), and (4), respectively, multiplied by the sphere volume.

For all studied configurations, results based on (1) and (3) are superimposed. The same is done with results based

on (2) and (4). It is possible to observe that the magnetic force is better described using H_{ext} than using H_{int} . Equations that use H_{int} present a large discrepancy from the experimental data, leading to a conclusion that (2) and (4) do not describe precisely the magnetic force.

In the “configuration a” [Fig. 6(a)] in the x interval of 0–5 mm, the analytical results using (1) and (3) closely agree with the experimental data. The remaining small discrepancy is explained by the approximations used to calculate the derivatives and the field and magnetization values [(6)–(9)]. However, in an overall evaluation, both (1) and (3) describe well the magnetic force acting on the steel sphere. Results obtained by the FEM analysis show a good similarity with the experimental data in this configuration.

“Configuration b” [Fig. 6(b)] presented the smallest values of magnetic force, and this can give a wrong impression of disagreement among the experimental and analytical curves. However, this disagreement is due to a poor signal-to-noise ratio in the measurements in this configuration, especially after the position 5 mm. If this aspect is considered, it is possible to say that (1) and (3) are still satisfactory. This conclusion is reinforced by the comparison of analytical, FEM, and experimental results. All results agree well with each other.

In the “configuration c” [Fig. 6(c)], a small disagreement is observed between the analytical results using (1) and (3) and the experimental data at the x interval from 0 to 5 mm. Even though, the phenomenon is well described. In addition, in this case, analytical results agree well with the FEM data.

The direct verification of the equations in experiment 1 indicates that (1) and (3) can give a very good prediction of the magnetic force for the three tested configurations. To confirm this conclusion, experiment 2 was made.

B. Experiment 2

No force was measured for up to 5 T in this experiment, and this indicates that a continuous gradient of magnetization cannot produce a magnetic force when a uniform magnetic field is applied in a ferromagnetic material. This disregards (1) and (2) as valid force descriptions to a body inside a region submitted to uniform applied field.

From the results of experiment 2, we conclude that the force appeared only in the presence of an applied field gradient.

V. CONCLUSION

The results of experiments conducted in this paper showed that (3) is the only one that can give a valid and precise description of the magnetic force for all studied cases. At least for soft magnetic materials, the derivative of magnetization does not produce any force for bodies submitted to uniform magnetic fields. This invalidates the equations related to the force of Liu for bodies submitted to a uniform applied field. The force appears only for bodies submitted to an applied field gradient, and the magnetic force is better described by using the external applied field instead of the internal field, like that established by the classic Kelvin’s formula.

ACKNOWLEDGMENT

This work was supported in part by the Coordenação de Aperfeiçoamento de Pessoal de Nível Superior, in part by the Fundação de Amparo à Pesquisa do Estado de São Paulo, and in part by the Conselho Nacional de Desenvolvimento Científico e Tecnológico. This work is dedicated to our deceased colleague Dr. I. da Silva.

REFERENCES

- [1] H. S. Choi, I. H. Park, and S. H. Lee, “Concept of virtual air gap and its applications for force calculation,” *IEEE Trans. Magn.*, vol. 42, no. 4, pp. 663–666, Apr. 2006.
- [2] S. Bobbio, F. Delfino, P. Girdinio, and P. Molfino, “Equivalent sources methods for the numerical evaluation of magnetic force with extension to nonlinear materials,” *IEEE Trans. Magn.*, vol. 36, no. 4, pp. 663–666, Jul. 2000.
- [3] A. Kitanovski and P. W. Egolf, “Thermodynamics of magnetic refrigeration,” *Int. J. Refrig.*, vol. 29, no. 1, pp. 3–21, 2006.
- [4] M. Balli *et al.*, “Réfrigération magnétique: Force magnétique,” Swiss Federal Office of Energy, Bern, Switzerland, Tech. Rep. 103,069, 2009.
- [5] R. Engel-Herbert and T. Hesjedal, “Calculation of the magnetic stray field of a uniaxial magnetic domain,” *J. Appl. Phys.*, vol. 97, no. 7, p. 074504, 2005.
- [6] A. Araujo, “Démagnétisation des pistons magnétocaloriques,” (in French), Bachelor Diploma Work, Thermal Sci. Eng. Inst., Univ. Appl. Sci., Yverdon-les-Bains, Switzerland, Tech. Rep., 2015.
- [7] K. Murakami and M. Nemoto, “Some experiments and considerations on the behavior of thermomagnetic motors,” *IEEE Trans. Magn.*, vol. 8, no. 3, pp. 387–389, Sep. 1972.
- [8] Y. Takahashi, T. Matsuzawa, and M. Nishikawa, “Fundamental performance of the disc-type thermomagnetic engine,” *Elect. Eng. Jpn.*, vol. 148, no. 4, pp. 26–33, Sep. 2004.
- [9] D. A. Gabrielyan, V. V. Semenov, and D. S. Martirosov, “Analysis of nonstationary heating and cooling of a thermomagnetic engine gadolinium working element,” *Russian Aeronautics*, vol. 56, no. 3, pp. 266–273, Dec. 2013.
- [10] D. Solomon, “Thermomagnetic mechanical heat engines,” *J. Appl. Phys.*, vol. 65, no. 9, p. 3687, 1989.